Open Porous Emulsion-Templated Monoliths: Effect of the Emulsion Preparation Conditions on the Foam Microstructure and Properties

Z. Abbasian, M. R. Moghbeli

School of Chemical Engineering, Iran University of Science and Technology, P. O. Box 16844, 13114 Tehran, Iran

Received 14 March 2009; accepted 7 September 2009
DOI 10.1002/app.31438
Published online 17 December 2009 in Wiley InterScience (www.interscience.wiley.com).

ABSTRACT: Highly open porous polymer foams were prepared via the polymerization of 10 : 1 styrene/divinylbenzene high-internal-phase emulsions (HIPEs) prepared under various emulsifying conditions. The effects of the emulsification stirring speed (SS) and rate of aqueous droplet-phase addition on the HIPE equilibrium torque value, an approximate characterization of HIPE viscosity, and the microstructure and properties of the resulting HIPE polymer solid foams were investigated. SS was varied over the range 400–1200 rpm for aqueous-droplet-phase addition rates (AARs) of 0.53 and 1.3 mL/min. The microscopic results showed that at lower AARs, increasing SS decreased the weighted-average cell diameter from 24.31 to 13.55 μm, whereas the cell size distribution was broadened, and the intercellular pore size varied irregularly in the range 0.76–1.42 μm. The average cell diameter and intercellular pore size for the solid foams prepared at higher AARs were greater than that of those prepared at lower AARs. The density of the foam materials ranged from 0.057 to 0.072 g/cm^3, whereas their thermal conductivity varied from 0.649 to 0.705 W m^{-1} °C^{-1}. The highest compressive stress–strain properties were found for the foam sample prepared with highest SS and a lower AAR. Adding electrolyte $CaCl_2$ to HIPE produced remarkable increases in the void diameter and intercellular pore size, especially at lower SS values. © 2009 Wiley Periodicals, Inc. J Appl Polym Sci 116: 986–994, 2010

Key words: emulsion polymerization; microstructure; polystyrene; templates

INTRODUCTION

Highly porous open-cell polymers, high-internal-phase emulsion polymer (polyHIPE) solid foams, are produced by the emulsion polymerization of the continuous organic phase of high-internal-phase emulsions (HIPEs), in which the internal phase occupies at least 74% of the emulsion volume.[1,2] These highly solid porous polymers have been prepared for various applications, such as catalyst supports, absorbents, filtration media, ion-exchange modules, separation media, tissue engineering applications, and chromatography because of the good control of the morphology.[3–8]

The pore size of a solid polymer foam reflects the droplet diameter in the emulsions and varies between 1 and around 100 μm.[9] The neighboring pores in the foams are connected via pore throats. Favorable pore and pore throat sizes and shapes can be achieved by the control of various variables, such as the surfactant and cosurfactant type and concentration, internal phase volume ratio, nature of organic phase, type of porogenic solvent, and electrolyte.[3–5,10,11] Williams[12] investigated the effect of oil-phase soluble types of porogenic solvents on the segregation and alignment of each molecular species during the polymerization of HIPEs made from styrene (St)/divinylbenzene (DVB)/dodecane using simple pictorial models. The results show that aromatic solvents interacted more strongly with the applied surfactant than the aliphatic ones. It is believed that solvents consisting of small aromatic molecules possess suitable nooks and, thus, provide a stabilizing influence by the elimination of empty regions. Only a limited range of formulations has been found; for instance, an optimal amount of surfactant is useful for making low-density foams of a monomer/surfactant/water tricomponent system.[13] In another piece of research, the relationship between the hydrophile–lipophile balance number of a cosurfactant and the stability of a St-based HIPE for several surfactants and cosurfactants was investigated.[14] Hainey et al.[15] studied the effect of the level of DVB and the use of a porogen in the oil phase on the microstructure of St/DVB polyHIPEs. Barbetta et al.[16] investigated the effect of the 4-vinyl benzyl

Correspondence to: M. R. Moghbeli (mr_moghbeli@iust.ac.ir).

TABLE I
Recipe for the Preparation of the PolyHIPE Polystyrene Foams

			Oil phase (g)			Aqueous phase (g)		
Code	SS	AAR	St	DVB	SMO	DDI	$K_2S_2O_8$	$CaCl_2$
1	400	0.52	1.812	0.181	0.4	39.671	0.08	0
2	600	0.52	1.812	0.181	0.4	39.671	0.08	0
3	800	0.52	1.812	0.181	0.4	39.671	0.08	0
4	1200	0.52	1.812	0.181	0.4	39.671	0.08	0
5	400	1.3	1.812	0.181	0.4	39.671	0.08	0
6	600	1.3	1.812	0.181	0.4	39.671	0.08	0
7	800	1.3	1.812	0.181	0.4	39.671	0.08	0
8	1200	1.3	1.812	0.181	0.4	39.671	0.08	0
9	400	1.3	1.812	0.181	0.4	39.671	0.08	0.249
10	600	1.3	1.812	0.181	0.4	39.671	0.08	0.249
11	800	1.3	1.812	0.181	0.4	39.671	0.08	0.249
12	1200	1.3	1.812	0.181	0.4	39.671	0.08	0.249

SS: stirring speed; AAR: aqueous-phase addition rate.

chloride (VBC) level on the morphology and average cell size of DVB/VBC polyHIPE solid foams. Their research showed that the decrease in the cell size of the polymers with increasing VBC content was due to the adsorption of VBC at the emulsion interface, which led to a lower interfacial tension and a smaller emulsion droplet size. They also investigated the morphology and surface area of polyHIPE foams prepared with oil-phase soluble porogenic solvents and Span80 surfactant in a three-component surfactant system.[17,18]

Although many scientists have investigated the effect of the emulsion composition on the polyHIPE microstructure and properties, less attention has been paid to the effect of the emulsification process parameters on the foam microstructure and properties. In this research, the effect of emulsification stirring speed (SS) and the rate of the addition of droplets in the aqueous phase on the HIPE viscosity and polyHIPE morphology and properties were investigated. In addition, we studied the effect of an electrolyte on the morphological aspects and mechanical properties of the resulting emulsion-templated foams prepared with various SS values.

EXPERIMENTAL

Materials

All reagents were purchased from Merck Co. (Darmstadt, Germany) unless otherwise stated. St was distilled *in vacuo* to remove inhibitors. DVB was purchased as a crosslinking agent and used without any further purification. Sorbitan monooleate (SMO; Span80) was prepared as an emulsifier. Potassium persulfate ($K_2S_2O_8$) and calcium chloride ($CaCl_2{\cdot}4H_2O$) were used as a water-soluble initiator and an electrolyte, respectively. Distilled deionized water (DDI) was prepared in our laboratory.

HIPE preparation

The organic phase of HIPE, containing St, DVB, and SMO, was poured into a 100-mL glass reactor equipped with a mechanical stirrer, nitrogen inlet, and condenser. The reactor was placed in a bath with thermostatic control. The St/DVB and monomer/SMO ratios in all of the emulsion samples were 90/10 and 80/20 (wt/wt), respectively. Table I shows the recipes of the HIPEs used to prepare the highly porous solid foams with various conditions. The aqueous phase was slowly added, drop by drop, to the continuous phase through a feeder at rates of 0.52 and 1.3 mL/min. SS was varied in the range 400–1200 rpm. After all of the internal phase was added, SS was held for a further 5 min to achieve a homogeneous foam emulsion.

HIPE torque measurement

The torque measurement provided an approximate characterization of the viscosity variations and emulsion stability during the HIPE preparation under various conditions. Software supplied with an RTZ Hidolf (Schwabach, Germany) overhead stirrer recorded the torque values of the HIPEs.

PolyHIPE preparation

The prepared HIPE samples were transferred to glass molds. After the molds were sealed, the emulsions were cured at 60°C in a circulating oven for 15 h. The polyHIPE solid foam materials were then dried *in vacuo* at 70°C for 48 h.

Characterization

PolyHIPE morphology

The morphology of the foam materials was studied by means of scanning electron microscopy (SEM). In

this case, the porous materials were frozen in liquid nitrogen; then, the fractured cross section was imaged. The fracture surface of the samples was gold-sputtered before microscopy. The average diameters of the voids and the intercellular pore sizes in the highly porous polymer samples were determined approximately from the SEM images on the basis of the size of 300 voids or pores for each sample.

PolyHIPE properties

The apparent density of the foams was determined from weight and volume measurements of the samples. The foam conductivity was measured on the basis of Fourier law with a thermal conductivity apparatus (PPM Co., Tehran, Iran). Compression tests were carried out according to ASTM D 1621-94. The samples were compressed to 75% of their initial height. The Young's modulus was determined from the initial linear slope of the stress–strain curve. In addition, the stress at yield was recorded to give the compression strength.

RESULTS AND DISCUSSION

The HIPEs were prepared with a constant internal phase volume fraction of 85% under various emulsifying operating conditions (Table I). The emulsification SS was varied from 400 to 1200 rpm for aqueous-droplet-phase addition rates (AARs) of 0.53 and 1.3 mL/min. In addition, HIPEs containing an electrolyte were also prepared with various SS values to investigate the role of the electrolyte on the morphology and properties of the resulting solid foams. A water-insoluble surfactant, Span80, was used at a constant 20% (wt/wt) relative to the continuous phase in all of the recipes (Table I).

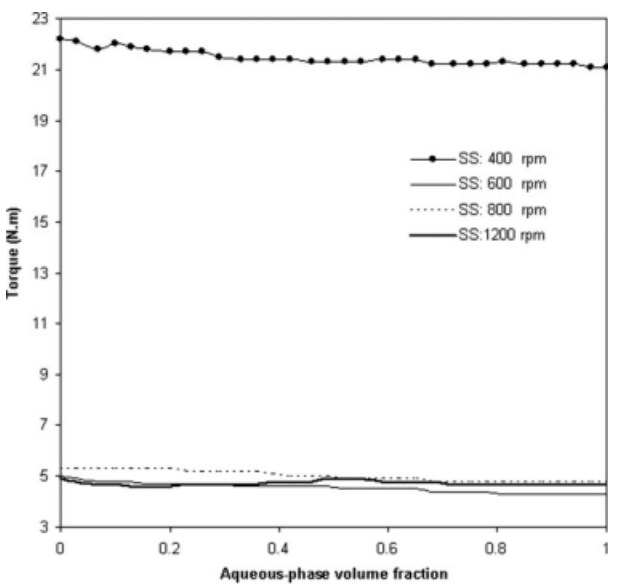

Figure 1 HIPE torque variations with increasing aqueous phase volume fractions at various SS values. AAR was 1.3 mL/min, and the concentrated emulsions were prepared without electrolyte.

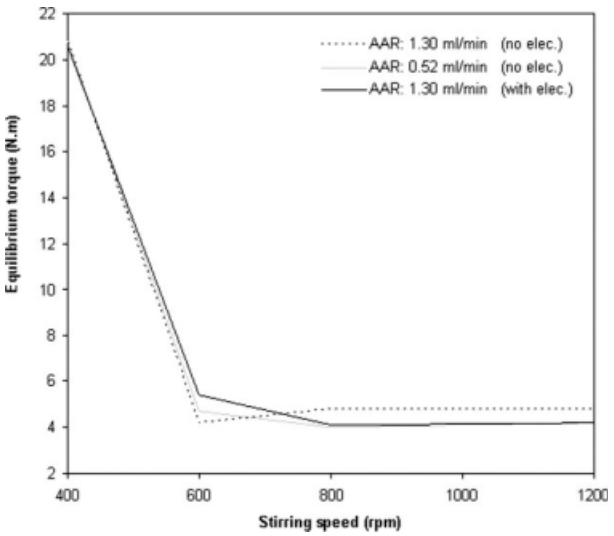

Figure 2 Effect of AAR and electrolyte (elec.) on the HIPE equilibrium torque versus SS.

HIPE torque variations

As mentioned earlier, the torque measurement versus aqueous volume fraction can provide approximate characterizations of the viscosity variation and emulsion stability during HIPE preparation for various emulsion preparation conditions. Figure 1 represents a typical example of the effect of SS on the variation of the HIPE torque with increasing aqueous volume fraction. As shown, at a given SS, the viscosity of the emulsifying system was approximately constant as the aqueous volume fraction increased with a constant feeding rate of 1.3 mL/min. This behavior may have been evidence of a stable emulsion preparation condition, in which the shear stress of the mixing process efficiently broke up the incoming aqueous phase to very fine droplets and rearranged them into a suitable close-packed configuration within the emulsifying mixture. Nevertheless, small torque fluctuations observed during the HIPE preparation, especially at higher internal phase volume fractions, were attributed to spontaneous break up and coalescence of the aqueous droplets. The effect of the AAR and the additional electrolyte on the HIPE equilibrium torque variations versus SS is shown in Figure 2. For the HIPEs prepared at higher and lower aqueous feeding rates, respectively, with and without electrolyte, the equilibrium torque was considerably reduced with an increase of

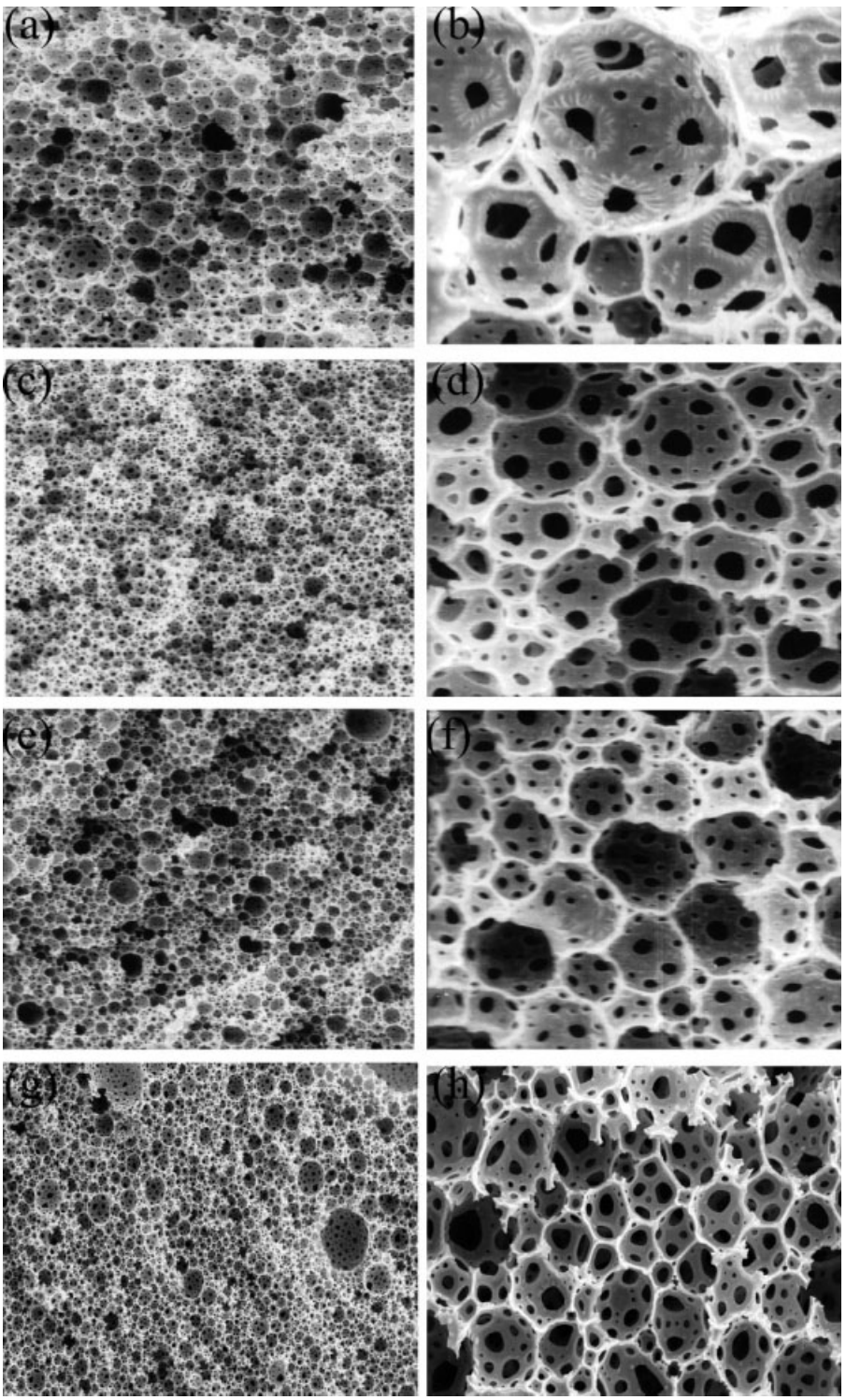

Figure 3 SEM micrographs of free-electrolyte polyHIPE foams prepared at various SS values and an AAR of 0.52 mL/min: (a,b) 400, (c,d) 600, (e,f) 800, and (g,h) 1200 rpm. (The magnifications of the left and right micrographs are 300 and 2000×, respectively.)

SS to 600 rpm, but beyond this limit, the torque values decreased slightly to a constant value. Small changes in the torque values observed at higher SS values could have been a result of an increase in the newly formed water–oil interfacial area, which compensated for the decrease of viscosity with increasing SS. Overall, one can imagine that increasing the SS not only lowered the emulsion viscosity and the size of the droplets completely enclosed by the organic phase but also caused the monomer/surfactant mixing films separating the adjacent emulsion droplets to become much thinner.

Interestingly, the same approximate viscosity values were observed for the former HIPE templates prepared at higher and lower aqueous-phase feeding rates, respectively, with and without electrolyte (Fig. 2). The use of the electrolyte to lower the interfacial tension between phases favored the dispersion of the internal phase and lowered the emulsion viscosity to the same extent obtained for the free-electrolyte HIPEs prepared at lower aqueous feeding rates; this provided sufficient mixing time to break up the droplets and redistribute the surfactant throughout the emulsifying system.

In contrast, at SS values over 600 rpm, the free-electrolyte emulsions prepared at higher aqueous feeding rates showed a higher emulsion viscosity than those prepared at lower feeding rates (Fig. 2). This behavior was attributed to the partial coagulation and instability occurring during the emulsification process, especially at higher SS values and AARs. Although the differences in the equilibrium torque of all the emulsions prepared at higher SS values were in the range 4–5 N m, any variation in the torque value was evidence of a change in the microstructure of the concentrated emulsions.

PolyHIPE morphology

The SEM micrographs clearly showed the effect of the emulsion SS on the microstructure of the free-electrolyte polyHIPE solid foams prepared with AARs of 0.52 and 1.3 mL/min (Figs. 3 and 4). An interconnected porous structure with cells, cell walls, and intercellular pores within the cell wall was observed in all of samples. At the lower AAR, increasing the SS considerably reduced the weight-average cell diameter (D_w), from 24.31 to 13.55 μm, whereas the cell-size distribution was broadened, and the intercellular pore size varied from 0.76–1.42 μm (Table II and Fig. 5). Increasing shear stress applied to the emulsifying mixture caused the low-viscosity system to efficiently break up the large aqueous phase to very finely dispersed droplets. Because the polyHIPE microstructure was a replica of the HIPE structure stabilized before gel formation,[17] a decrease in the emulsion droplet size and, consequently, a decrease in the foam void diameter was observed as SS increased (Fig. 3). Nevertheless, the nonuniform shear stress field created around the stirrer impeller and partial coalescence arose from the rupture of the liquid thin film between the adjacent small droplets and resulted in a bimodal void size distribution in the resulting solid foams. On the other hand, the microscopic observations implied that the three-dimensional packing of the enclosed droplets in the HIPEs was more compact when SS increased [Fig. 3(f,h)]. As shown, a further increase in SS seemed to lead to the deformation of a large number of enclosed small droplets and, consequently, to an interconnected hexagonal packed-cell arrangement. Figure 6 shows a schematic representation of the effect of the emulsification operating conditions on the microstructure of the resulting solid foams. In addition, an increase in the degree of cell interconnection, as expressed here by the number-average intercellular pore size (d_w)/number-average cell diameter (D_n) ratio, was observed with increasing SS (Table II). The geometry of the intercellular pore throats changed from trapezoidal to spherical or ellipsoidal as SS increased (Fig. 3).

The average cell diameter and intercellular pore or interconnecting window size for the polyHIPE solid foams prepared at higher droplet-phase feeding rates were greater than those of the solid foams prepared at lower AARs (Table II and Fig. 4). In this case, increasing SS decreased the weighted-average cell diameter from 40.22 to 15.25 μm and reduced the intercellular pore size from 3.74 to 1.19 μm (Fig. 5). The pore size in the emulsion templates prepared at a constant surfactant level and internal phase volume fraction with various emulsification process parameters was connected to the size and geometric conformation of the enclosed droplets within the emulsion. Increasing the number of small droplets and water–oil interfacial area with increasing SS and decreasing AAR led to a decrease in the surfactant concentration within the continuous thin organic film separating the adjacent emulsion droplets. A lower surfactant level within the oil phase layer resulted in a less developed separation phase within the polymerizing organic layer and finally formed smaller intercellular windows (Figs. 3 and 4). Nevertheless, an increased intercellular pore density was observed when SS increased because of the increase in the area of contact points of deformed neighboring droplets. On the other hand, the increase of SS up to 800 rpm broadened the cell size distribution, but beyond this limit, the cell size polydispersity decreased. In fact, partial emulsion instability occurred with increasing SS and AAR enhanced the polydispersity of the cell diameter in the polymerized emulsion templates (Table II).

Figure 7 indicates the effect of the electrolyte on the morphology of the solid foams whose concentrated emulsions were prepared at various SS values. As shown, the addition of the electrolyte to the aqueous phase caused a remarkable increase in the interconnecting window size and interconnectivity in the emulsion foams, compared to the corresponding foams prepared without electrolyte (Figs. 4 and 7). The explanation is that an increase in the window size brought about by the addition of the electrolyte was a result of a decrease in the

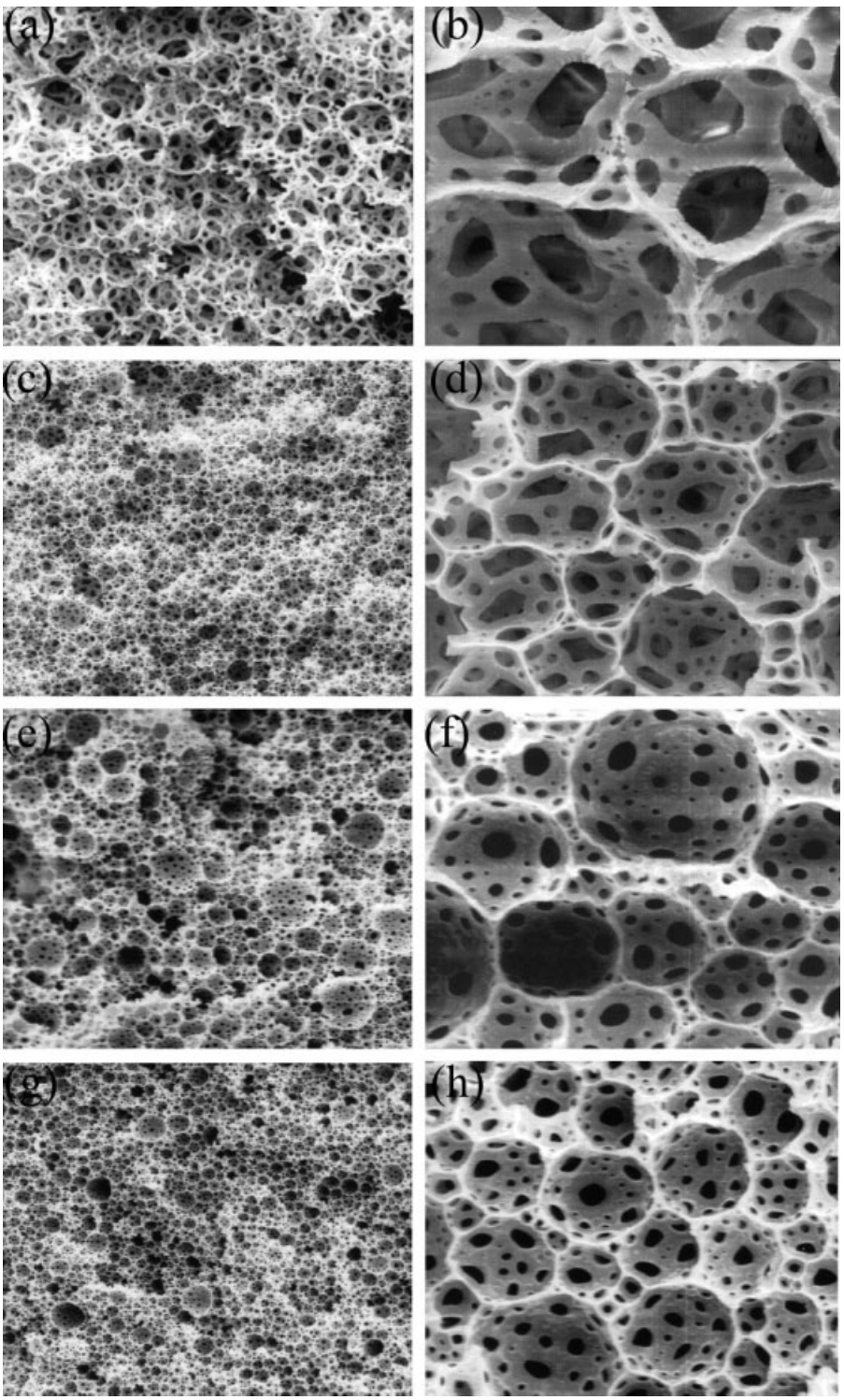

Figure 4 SEM micrographs of free-electrolyte polyHIPE foams prepared at various SS values and an AAR of 1.3 mL/min: (a,b) 400, (c,d) 600, (e,f) 800, and (g,h) 1200 rpm. (The magnifications of the left and right micrographs are 300 and 2000×, respectively.)

interfacial tension and, consequently, a decrease in the oil film thickness between adjacent droplets to the critical film thickness, which caused it to form windows on polymerizing. On the other hand, although an increase in the stirring rate up to 600 rpm considerably decreased the window diameter, beyond this limit, no significant change in size was observed (Fig. 5). In addition, the electrolyte caused a reduction in the tendency for Ostwald ripening and progressive coarsening of the emulsion,

TABLE II
Characteristics of the Prepared PolyHIPE Foams

Code	D_n (μm)	D_w (μm)	PDI	d_w (μm)	d_w/D_n	ρ (g/cm^3)	κ (W m^{-1} k^{-1})	E (MPa)	σ_{cr} (MPa)
1	15.12	24.31	1.61	1.42	0.106	0.062	0.705	4.054	0.049
2	8.70	14.27	1.64	1.39	0.160	0.071	0.694	4.257	0.161
3	7.32	14.58	1.99	0.76	0.104	0.072	0.686	6.747	0.205
4	6.27	13.55	2.16	1.18	0.188	0.067	0.665	11.456	0.231
5	27.03	40.22	1.49	3.74	0.138	0.071	0.655	5.199	0.128
6	12.24	18.72	1.53	1.51	0.123	0.069	0.658	5.803	0.072
7	9.81	31.34	3.20	1.49	0.152	0.064	0.697	8.117	0.176
8	7.05	15.25	2.16	1.19	0.169	0.062	0.653	9.140	0.201
9	46.78	64.29	1.37	8.27	0.177	0.068	0.665	2.833	0.074
10	13.36	17.99	1.35	2.87	0.215	0.062	0.664	9.194	0.089
11	11.41	18.42	1.61	2.90	0.254	0.057	0.649	3.412	0.129
12	8.81	15.94	1.81	2.90	0.329	0.064	0.617	4.403	0.113

D_n = number-average cell diameter; D_w = weight-average cell diameter; d_w = number-average intercellular pore size; ρ = foam density; κ = foam thermal conductivity; E = Young's modulus; σ_{cr} = crush strength.

conditions that would result in a narrow window size distribution (Fig. 7).

PolyHIPE physical properties

As previously described, the cell structures of the solid foams prepared with various emulsifying conditions were quite different. The density, thermal conductivity, and compressive properties of the solid foams with different microcellular structures are listed in Table II. The foam density varied from 0.057 to 0.072 g/cm^3, whereas the thermal conductivity ranged from 0.649 to 0.705 W m^{-1} °C^{-1}. An increase in the foam density and a decrease in the thermal conductivity values were observed for the foam materials prepared at lower AARs and at enhanced SS values. An inverse effect was observed for the foams prepared at higher AARs without the electrolyte (Table II). Interestingly, both the foam density and thermal conductivity decreased with increasing SS for the foams prepared with the electrolyte at higher AARs.

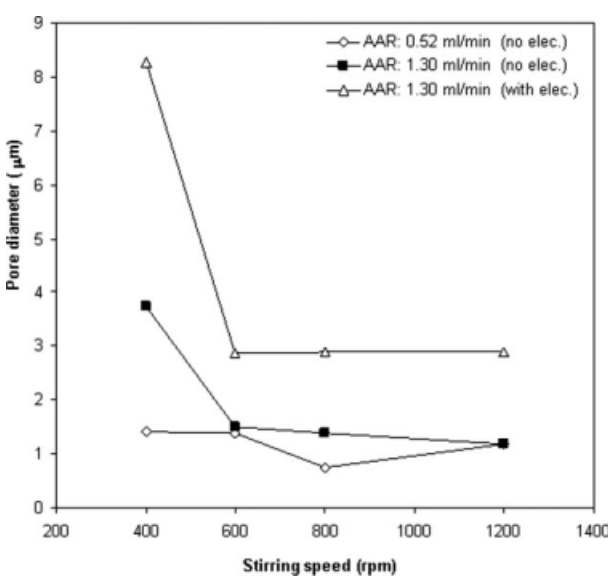

Figure 5 Effect of various emulsion preparation conditions on the pore diameter of the resulting solid foams (elec. = electrolyte).

PolyHIPE mechanical properties

The room compression properties of all of the 10 : 1 St/DVB polyHIPE foams with various microstructures are shown in Table II. All of the emulsion foams had three-stage compressive stress–strain curves typical of polyHIPE foams, a linear stress–strain region, a stress plateau region, and a densification region showing a steep increase in stress (Figs. 8 and 9). All of the foam samples compressed smoothly until the limit of the compression cell was reached. As shown, varying the emulsifying

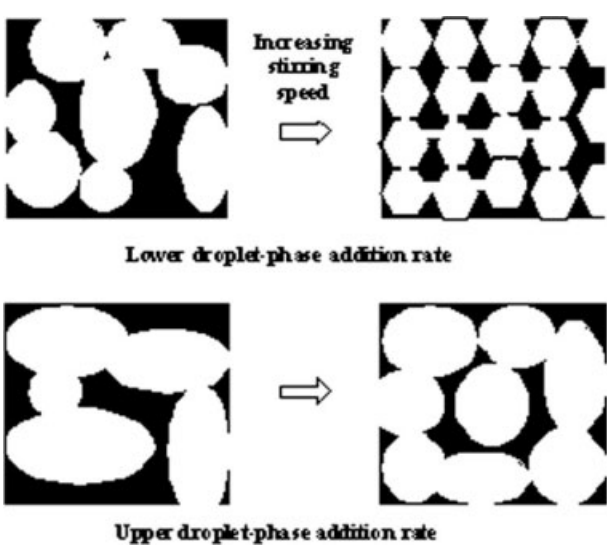

Figure 6 Schematic foam microstructures prepared under various emulsion preparation conditions.

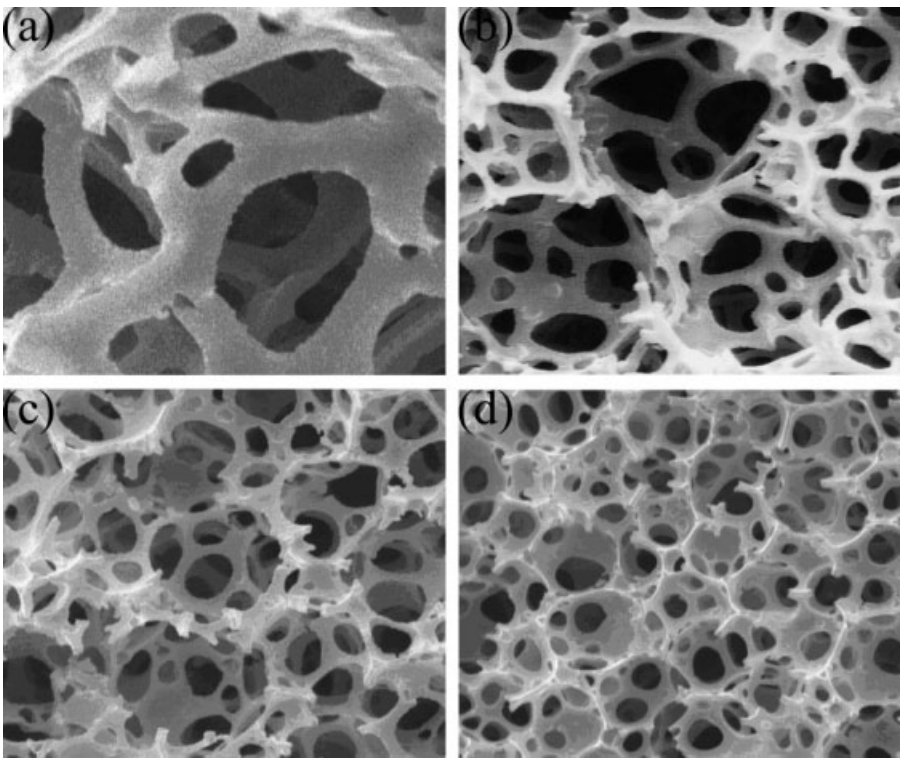

Figure 7 Effect of electrolyte on the microstructure of the foams prepared at various SS values: (a) 400, (b) 600, (c) 800, and (d) 1200 rpm (AAR = 1.3 mL/min).

conditions considerable influenced the Young's modulus and crush and ultimate strengths of the emulsion foams. Increasing SS by lowering the cell size and the associated compaction caused the Young's modulus and crush strength to increase considerably (Figs. 8 and 9). In fact, the foam materials with smaller cell sizes and thinner intercellular wall thicknesses prepared at higher SS values showed more compact interconnected porous structures and higher compressive properties. In contrast, increasing AAR and adding electrolyte decreased the foam compressive properties (Table II). This behavior was attributed to the increase in the cell and pore sizes in the foams as AAR increased (Fig. 6). Increasing

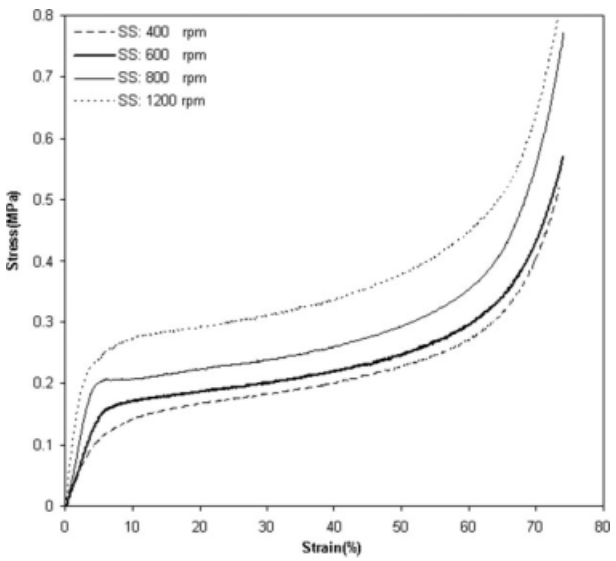

Figure 8 Compressive stress–strain curves of polyHIPE foams prepared at various SS values. AAR was 0.52 mL/min, and the resulting foams were prepared without electrolyte.

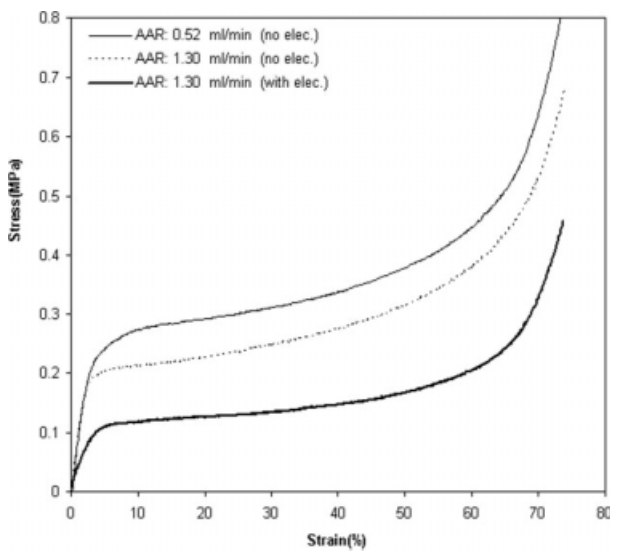

Figure 9 Effect of AAR and electrolyte (elec.) on the foam compression properties (SS = 600 rpm).

the wall thickness and moduli and higher pore connectivity in the previous foams with coarse open-cell structures resulted in more brittleness. However, the highest compressive properties belonged to the foam sample prepared with the highest SS and the lower AAR. In this case, a more compact hexagonal open-cell structure with flat borders between neighboring cells was obvious [Fig. 3(h)].

CONCLUSIONS

The 10 : 1 St/DVB HIPEs were prepared with a constant internal phase volume fraction of 85%. The effects of the emulsification operating conditions, SS and AAR, on the emulsion viscosity, morphology, and compression properties of the resulting solid foams were investigated. For all of the HIPEs prepared at higher and lower AARs, the equilibrium torque was considerably reduced with increasing SS up to 600 rpm, but beyond this limit, the torque values varied slightly to achieve a constant amount in the range 4–5 N m. The foam microstructure was dependent on the intensity of the applied shear stress, AAR, and addition of electrolyte during the emulsification process. At a given AAR, increasing the SS from 600 to 1200 rpm considerably decreased the void diameter in the range 64.29–15.94 μm, especially for the emulsions prepared with electrolyte. However, the results imply that lowering the cell size in the resulting solid foams increased SS of the prepared emulsions. The foam density varied from 0.057 to 0.072 g/cm^3, whereas the thermal conductivity ranged from 0.649 to 0.705 W m^{-1} °C^{-1}. Increasing SS by lowering the cell size and the associated compaction caused the Young's modulus and crush strength to increase considerably. In contrast, the increase in AAR and the addition of electrolyte decreased the foam compressive properties.

References

1. Cameron, N. R. Polymer 2005, 46, 1439.
2. Cameron, N. R.; Sherrington, D. C. Adv Polym Sci 1996, 126, 163.
3. Barbetta, A.; Carnachan, R. J.; Smith, K. H.; Zhao, C. T.; Cameron, N. R.; Kataky, R.; Hayman, M.; Przyborski, S. A.; Swan, M. Macromol Symp 2005, 226, 203.
4. Williams, J. M. Langmuir 1991, 7, 1370.
5. Williams, J. M.; Wrobleski, D. A. Langmuir 1988, 4, 656.
6. Krajnc, P.; Leber, N.; Stefanec, D.; Kontrec, S.; Podgornik, A. J Chromatogr A 2005, 1065, 69.
7. Cetinkaya, S.; Khosravi, E.; Thompson, R. J Molecular Catal A 2006, 254, 138.
8. Pulko, I.; Kolar, M.; Krajnc, P. Sci Total Environ 2007, 386, 114.
9. Akay, G.; Birch, M. A.; Bokhari, M. A. Biomaterials 2004, 25, 3991.
10. Busby, W.; Cameron, N. R.; Jahoda, C. Biomacromolecules 2001, 2, 154.
11. Wakeman, R. J.; Bhumgara, Z. G.; Akay, G. Chem Eng J 1998, 70, 133.
12. Williams, J. M. Langmuir 1988, 4, 44.
13. Williams, J. M.; Wrobleski, D. A. Langmuir 1988, 4, 656.
14. Williams, J. M. Langmuir 1991, 7, 1370.
15. Hainey, P.; Huxham, I. M.; Rowatt, B.; Sherrington, D. C.; Tetley, L. Macromolecules 1991, 24, 117.
16. Barbetta, A.; Cameron, N. R.; Cooper, S. J. Chem Commun 2000, 3, 221.
17. Barbetta, A.; Cameron, N. R. Macromolecules 2004, 37, 3188.
18. Barbetta, A.; Cameron, N. R. Macromolecules 2004, 37, 3202.